ChemPubSoc Europe

DOI: 10.1002/chem.201701855

CHEMISTRY
A European Journal
Communication

C–H Activation

A 1,2-Addition Pathway for C(sp^2)–H Activation at a Dinickel Imide

Ian G. Powers,[a] Cholpisit Kiattisewee,[a] Kimberly C. Mullane,[b] Eric J. Schelter,[b] and Christopher Uyeda*[a]

Abstract: A dinickel imido complex was synthesized using a redox-active naphthyridine-diimine supporting ligand. Upon coordination of an external ligand, the Ni_2 core was disrupted, triggering an aromatic C–H activation reaction to generate a Ni_2(μ-NHAr)(Ar) species. This intermediate is capable of liberating free carbazole and phenanthridine products upon heating or treatment with excess *t*BuNC. Collectively, these studies establish a kinetically facile 1,2-addition mechanism for C(sp^2)–H activation, taking advantage of cooperative reactivity between two Ni centers.

Transition-metal nitrene (imido) complexes have attracted significant interest as synthetic targets due to their proposed role in C–H amination reactions.[1] Late transition-metal terminal nitrenes, relevant to several catalytic processes,[2] are inherently challenging to isolate and characterize owing to the absence of strong metal–ligand multiple bonding. Nevertheless, noteworthy examples have been reported using supporting ligands that provide steric protection and enforce low coordination numbers.[3] Mechanistic studies have revealed two predominant pathways by which transition-metal-bound nitrenes can insert into C–H bonds: concerted reactions involving a three-centered transition state and stepwise sequences of H-atom abstraction followed by radical recombination. In both mechanisms, the metal center participates electronically by supplying oxidizing equivalents but does not directly interact with the C–H bond being cleaved. As a consequence of this ligand-based mechanism, transition-metal nitrenes often behave similarly to free nitrenes, exhibiting selectivities that are highly correlated with relative C–H bond dissociation energies.

Our group is interested in capitalizing on the electronic properties of metal–metal bonds to uncover new mechanisms for organometallic transformations. In this context, we recently described a [NDI]Ni_2 (NDI = naphthyridine-diimine) platform capable of promoting redox reactions across the Ni_2 fragment by reversibly storing electron density in the NDI extended π-system.[4] Here, we report a structurally characterized Ni_2 bridging imido complex that cleaves aromatic C–H bonds at room temperature by a 1,2-addition mechanism.[5] This reactivity highlights an organometallic C(sp^2)–H activation pathway that takes advantage of the direct participation of two metals and contrasts with the ligand-based mechanisms commonly observed using mononuclear terminal imido complexes.

We initiated our studies by pursuing the synthesis of a stable nitrene complex using an organic azide precursor and the [^{iPr}NDI]Ni_2(C_6H_6) complex (**1**) as a low-valent dinickel synthon. Treatment of **1** with *m*-terphenylazide (1.0 equiv) results in the immediate evolution of N_2 gas and the clean formation of a new paramagnetic species (**2**), which undergoes gradual decomposition to NMR-silent products when stored in C_6D_6 at room temperature (Figure 1a). Despite its instability in solution, single crystals of **2** may be obtained from pentane at −30 °C, enabling its unambiguous characterization by XRD as the authentic mononitrene species (Figure 1b). In the solid state, the μ-NAr ligand is displaced from the mean [N_4]Ni_2 plane and symmetrically bridges the two Ni centers. The Ni–N(Ar) distances are relatively short at 1.768(2) and 1.784(3) Å, and the N(Ar) atom adopts a nearly planar geometry as mea-

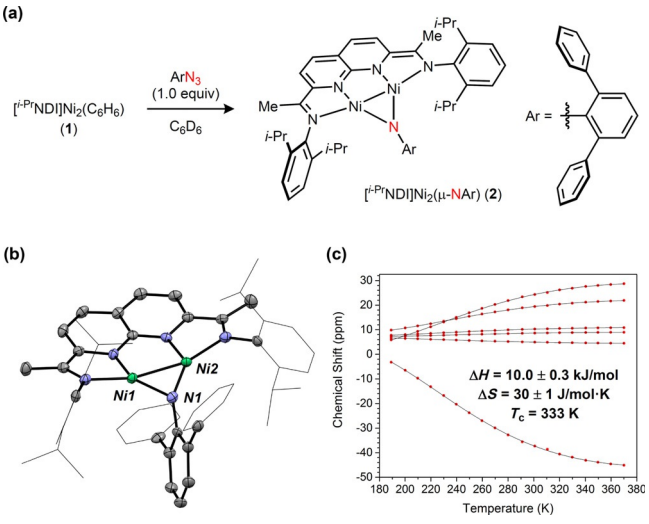

Figure 1. (a) Synthesis and (b) solid-state structure of [^{iPr}NDI]Ni_2(NAr) (**2**, Ar = 2,6-$(Ph)_2C_6H_3$-). Ni1–Ni2: 2.3415(9) Å. (c) Variable-temperature ^{1}H NMR chemical-shift data for **2** over a temperature range of 190–370 K, with thermodynamic parameters for the spin equilibrium.

[a] I. G. Powers, C. Kiattisewee, Prof. C. Uyeda
Department of Chemistry, Purdue University
560 Oval Dr., West Lafayette, IN 47907 (USA)
E-mail: cuyeda@purdue.edu

[b] K. C. Mullane, Prof. E. J. Schelter
Department of Chemistry, University of Pennsylvania
231 S. 34th St. Philadelphia, PA 19104 (USA)

Supporting information and the ORCID identification number(s) for the author(s) of this article can be found under https://doi.org/10.1002/chem.201701855.

sured by the sum of the angles around nitrogen of 345.0(5)°. These metrics are suggestive of net π-bonding between the Ni–Ni bond and the NAr ligand.

The μ-NAr complex **2** exhibits temperature-dependent paramagnetism in solution (Figure 1c).[3b,f,6] At 298 K, the effective magnetic moment was determined by the Evans method to be 1.64 μ_B, a value that is intermediate between the expected value for an $S=0$ and an $S=1$ state. To probe this magnetic behavior, ^{1}H NMR spectra of **2** were examined over a broad temperature range of 190–370 K in [D_8]toluene. At low temperatures, the chemical shifts are found near their diamagnetic range. At higher temperatures, the resonances become increasingly paramagnetically shifted, indicating population of a higher spin state. Thermodynamic parameters for the spin equilibrium were extracted by modeling these data according to a mixture of singlet and triplet states. The enthalpy term is relatively small and favors the singlet by 10.0 ± 0.3 kJ mol^{-1}; the triplet is favored entropically by 30 ± 1 J mol^{-1} K^{-1}, leading to its predominance at higher temperatures. The three most paramagnetically shifted ^{1}H NMR resonances appear at 29, 22, and −45 ppm at 370 K and were assigned as the imine methyl substituent and naphthyridine protons. The large shift in these peaks implicates the redox-active π-system of the NDI ligand as a significant contributor to overall spin density in the triplet state.

DFT calculations provide insight into the bonding between the imido and Ni_2 fragments in complex **2** (Figure 2a). In the $S=0$ state, the Ni–Ni π-bonding combination mixes with the unhybridized N(Ar) *p*-orbital to form a three-center, two-electron π-interaction polarized toward nitrogen. The corresponding Ni_2-NAr *anti*-bonding combination is the LUMO for the complex. The HOMO is Ni–Ni(π*) in character and is delocalized into the π-system of the NDI ligand. In the $S=1$ state, an electron is promoted from the HOMO to the LUMO, resulting in spin density that is distributed over the NDI ligand, the Ni–Ni bond, and the nitrogen *p*-orbital (Figure 2b).

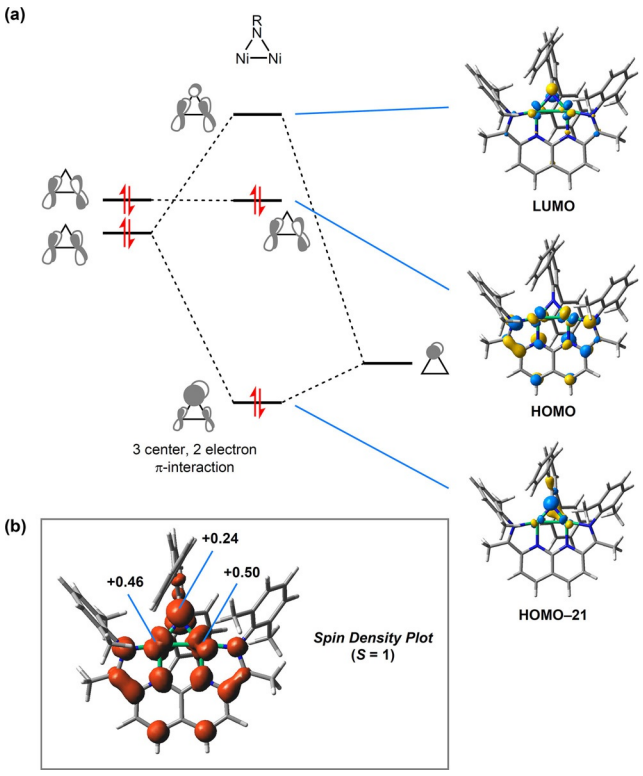

Figure 2. (a) Select Kohn–Sham orbitals for **2** highlighting interactions relevant to bonding in the Ni_2(μ-NR) fragment. (b) A spin-density plot for the $S=1$ spin state of **2**.

Attempts to induce nitrene transfer from **2** led to the observation of a competing intramolecular C(sp^2)–H activation process (Figure 3a).[7] The reaction of **2** with *t*BuNC yields a C_1-symmetric product **3**, assigned by XRD as the aryl amido complex resulting from 1,2-addition of an *ortho* C–H group across a Ni–(μ-NAr) bond (Figure 3b). The N(H)(Ar) atom maintains its bridging configuration but exhibits elongated Ni–N distances (1.93(1) and 1.850(9) Å) relative to the imido precursor **2**. The isonitrile and the aryl ligands are terminally coordinated to different Ni centers and located in the [N_4]Ni_2 plane. The Ni–Ni distance is elongated to 3.041(2) Å, suggesting a substantial weakening of the metal–metal interaction. At room temperature, no detectable magnetic moment is observed for **3**, and a majority of the ^{1}H NMR resonances fall within the diamagnetic envelope; however, the presence of three upfield-shifted signals at −5, −9, and −13 ppm suggests a small degree of mixing from a higher-energy triplet state. According to the variable temperature ^{1}H NMR data, the triplet is disfavored en-

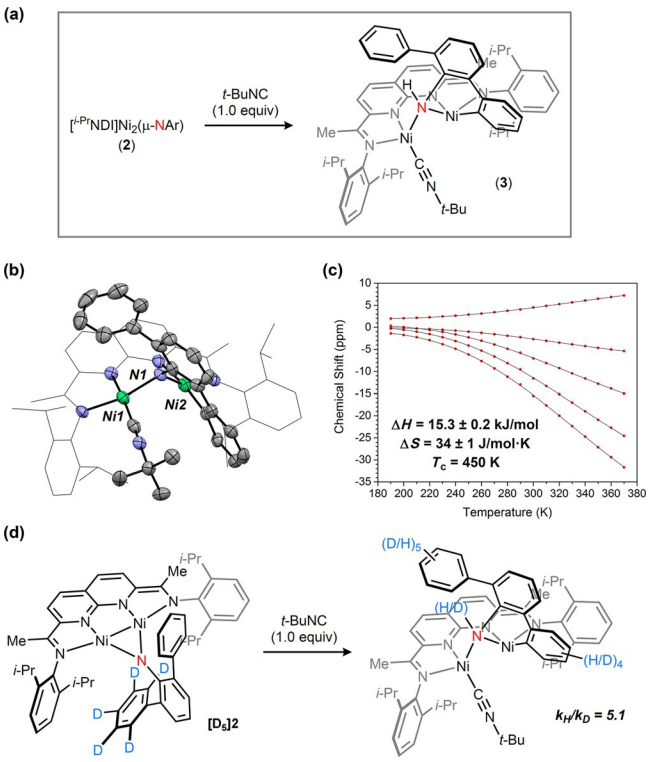

Figure 3. (a) An isonitrile-induced 1,2-addition of a C–H bond from **2**. (b) Solid-state structure of **3**. (c) Variable-temperature ^{1}H NMR chemical-shift data for **3** over a temperature range of 190–370 K, with thermodynamic parameters for the spin equilibrium. (d) Kinetic isotope effects measurement for the C–H activation using the H/D-competition substrate [$\mathbf{D_5}$]**2**.

thalpically by 15.3 ± 0.2 kJ mol^{-1}, and 89% of **3** is in its singlet state at room temperature (Figure 3c).

The observed reactivity of **2** is unusual in that transition-metal imido complexes, regardless of their nuclearity, are generally found to react with isonitriles by simple nitrene transfer to form carbodiimides. For example, Hillhouse[8] and Warren[9] reported the synthesis of $Ni_2(\mu\text{-NAr})$ species that cleanly react with *t*BuNC to generate the corresponding *t*BuNCNAr product in high yield. We hypothesized that the constrained dinuclear environment enforced by the NDI chelating ligand might be serving to disfavor migratory insertion of isonitrile and instead place an aromatic C–H bond in a favorable orientation to undergo activation. As a point of comparison, the dimeric $[(bpy)Ni(\mu\text{-NAr})]_2$ complex **4** bears the same *m*-terphenylimido fragment as that found in **2** but cleanly reacts with *t*BuNC to form the carbodiimide **5** (91% yield) with no detectable C–H activation products (Figure 4).

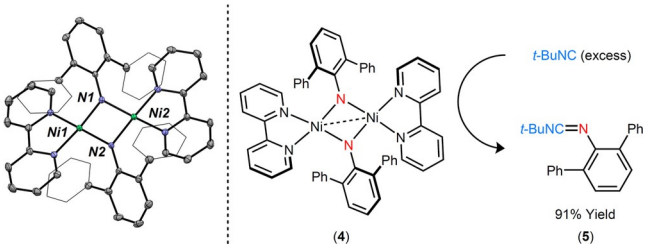

Figure 4. (a) Solid-state structure of **4** (Ni1–Ni2: 2.8201(5) Å). (b) Nitrene transfer reactivity with *t*BuNC to form the carbodiimide product **5**.

In order to further probe the mechanism of the C–H activation, the nitrene complex **[D$_5$]2**, containing isotopically differentiated phenyl substituents, was prepared (Figure 3d). Upon treatment with *t*BuNC (1.0 equiv), a mixture of two isotopomers was obtained, and a k_H/k_D of 5.1 was determined from the product ratio. The large primary kinetic isotope effect (KIE) value is indicative of C–H bond cleavage in the rate-determining transition state. By contrast, KIE values of $\leq$1.7 have been observed in catalytic C(sp^2)–H amination reactions that are proposed to involve an electrocyclization mechanism where C–N bond formation is followed by a rapid 1,2-hydride shift.[10]

The elementary steps in the 1,2-addition pathway were further examined using DFT calculations (Figure 5). The initial coordination of the isonitrile ligand is highly exothermic and induces cleavage of the Ni–Ni bond (Ni–Ni: 3.17 Å in intermediate A). To satisfy its coordination sphere, the Ni center not bearing the isonitrile forms an η^2 interaction with one of the phenyl groups of the *m*-terphenylimido ligand. C–H activation is preceded by reorientation of the phenyl group to form a C–H σ-complex (B), which is 23.6 kJ mol^{-1} higher in energy. From intermediate B, the activation energy for 1,2-addition is only 27.6 kJ mol^{-1}, corresponding to an overall barrier of 51.2 kJ mol^{-1} from A to TS1. The initial amido aryl intermediate C is nearly isoenergetic to A but is capable of rotating to the more stable isomer D, which corresponds closely to the XRD structure of complex **3**. By comparing the zero-point vibrational energies for the C–H and C–D activation processes, a KIE

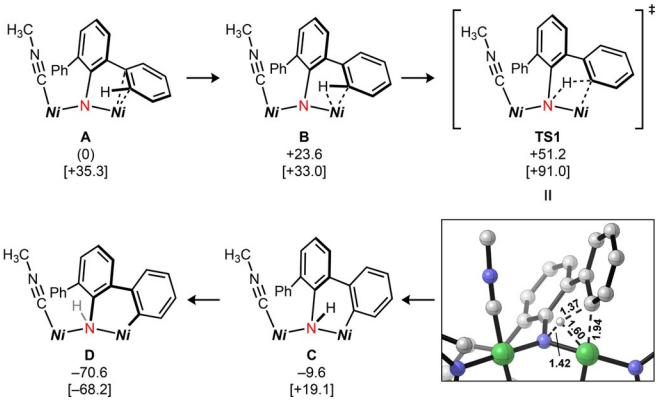

Figure 5. Calculated reaction coordinate for the C–H activation reaction. Free energies (ΔG) on the singlet surface are shown in kJ mol^{-1} (ΔG values on the triplet surface are in square brackets). All ΔG values are relative to the energy of A in the singlet state. The *i*Pr groups on the NDI ligand and the *t*Bu group on the isonitrile were truncated to methyl groups.

value of 4.5 was calculated, in agreement with the value obtained experimentally. The pathway leading to carbodiimide formation was also calculated, and the barrier to migratory insertion of isonitrile into the Ni–(μ-NAr) bond was found to be 48.5 kJ mol^{-1} higher in energy than the C–H activation barrier.

The 1,2-addition of a C–H bond to a M=NR species has only previously been observed for coordinatively unsaturated Ti^{IV}[11] and Zr^{IV}[12] imides. For these early transition metal complexes, the thermodynamic driving force to maintain a d^0 electronic configuration imposes prohibitive barriers to C–N reductive elimination. Motivated by the observation of 1,2-addition reactivity in a late transition-metal system, we examined the possibility of generating C–H aminated products from **3** (Figure 6). Addition of excess *t*BuNC to **3** causes the immediate release of the phenanthridin-6(5*H*)-imine **6**, which undergoes tautomerization over 1 h at room temperature to form the more stable phenanthridine product **7** (90% yield). Alternatively, thermolysis of **3** in C_6D_6 at 80 °C for 5 d generates a mixture of **7** and 1-

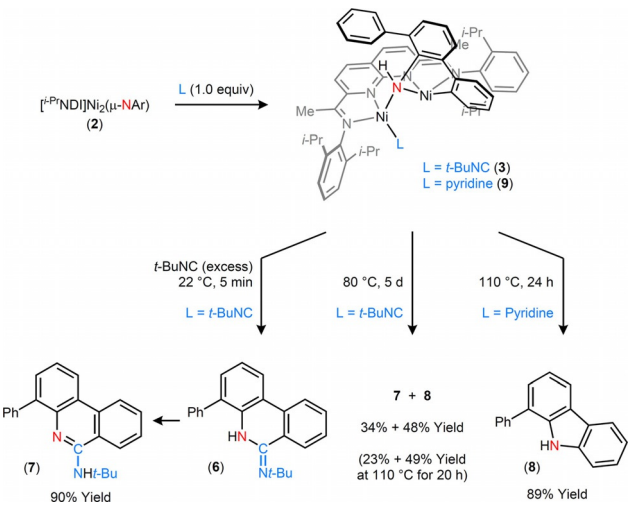

Figure 6. Thermal and *t*BuNC-induced reductive elimination reactions to generate carbazole and phenanthridine products.

phenylcarbazole (**8**),[13] indicating that the direct C–N reductive elimination competes with migratory insertion of *t*BuNC. Following the thermal reaction, [^{iPr}NDI]$Ni_2(C_6D_6)$ (**1**) is regenerated in 43% yield, demonstrating a complete synthetic cycle for the conversion of *m*-terphenylazide to aminated heterocycle products.[14] We hypothesized that the use of an alternative coordinating ligand, incapable of undergoing migratory insertion, might yield exclusively the carbazole product (**8**). Accordingly, addition of pyridine (4 equiv) to **2** produces a C–H activated complex (**9**), which, upon heating at 110 °C for 24 hours, eliminates **8** in 89% yield.

In summary, we have identified an isolable dinickel bridging imido complex (**2**) capable of accessing diamagnetic and paramagnetic states through thermally induced spin crossover. Upon coordination of an external ligand such as *t*BuNC, the Ni–Ni interaction is destabilized, initiating a kinetically facile aromatic C–H bond activation by a 1,2-addition mechanism. This reactivity can be coupled with reductive elimination reactions to achieve high-yielding syntheses of carbazole and phenanthridine heterocycles. Together, these studies demonstrate that multinuclear nitrenes, often viewed as being relatively inert compared to their terminal counterparts, can access unique pathways for functionalizing C–H bonds.

Acknowledgements

This research was supported by the U.S. National Science Foundation (CHE-1554787) and Purdue University. We thank Dr. Matthias Zeller for assistance with XRD experiments. E.J.S. thanks the U.S. National Science Foundation (CHE-1362854), and C.K. thanks the Faculty of Science at Mahidol University for financial support. C.U. is an Alfred. P. Sloan Research Fellow and I.G.P. is an NSF Graduate Research Fellow.

Conflict of interest

The authors declare no conflict of interest.

Keywords: amination · C–H activation · metal–metal interactions · nickel · nitrene

[1] a) C. G. Espino, J. Du Bois, in *Modern Rhodium-Catalyzed Organic Reactions*, Wiley-VCH, Weinheim, **2005**, pp. 379–416; b) H. M. L. Davies, J. R. Manning, *Nature* **2008**, *451*, 417–424; c) F. Collet, R. H. Dodd, P. Dauban, *Chem. Commun.* **2009**, 5061–5074; d) K. Shin, H. Kim, S. Chang, *Acc. Chem. Res.* **2015**, *48*, 1040–1052.

[2] a) S. K.-Y. Leung, W.-M. Tsui, J.-S. Huang, C.-M. Che, J.-L. Liang, N. Zhu, *J. Am. Chem. Soc.* **2005**, *127*, 16629–16640; b) Y. M. Badiei, A. Dinescu, X. Dai, R. M. Palomino, F. W. Heinemann, T. R. Cundari, T. H. Warren, *Angew. Chem. Int. Ed.* **2008**, *47*, 9961–9964; *Angew. Chem.* **2008**, *120*, 10109–10112; c) V. Lyaskovskyy, A. I. O. Suarez, H. Lu, H. Jiang, X. P. Zhang, B. de Bruin, *J. Am. Chem. Soc.* **2011**, *133*, 12264–12273; d) R. H. Perry, T. J. Cahill, J. L. Roizen, J. Du Bois, R. N. Zare, *Proc. Natl. Acad. Sci. USA* **2012**, *109*, 18295–18299; e) Y. Liu, X. Guan, E. L.-M. Wong, P. Liu, J.-S. Huang, C.-M. Che, *J. Am. Chem. Soc.* **2013**, *135*, 7194–7204; f) A. Varela-Álvarez, T. Yang, H. Jennings, K. P. Kornecki, S. N. Macmillan, K. M. Lancaster, J. B. C. Mack, J. Du Bois, J. F. Berry, D. G. Musaev, *J. Am. Chem. Soc.* **2016**, *138*, 2327–2341.

[3] For examples of first-row late transition-metal imido complexes: a) D. J. Mindiola, G. L. Hillhouse, *J. Am. Chem. Soc.* **2001**, *123*, 4623–4624; b) D. T. Shay, G. P. A. Yap, L. N. Zakharov, A. L. Rheingold, K. H. Theopold, *Angew. Chem. Int. Ed.* **2005**, *44*, 1508–1510; *Angew. Chem.* **2005**, *117*, 1532–1534; c) E. Kogut, H. L. Wiencko, L. Zhang, D. E. Cordeau, T. H. Warren, *J. Am. Chem. Soc.* **2005**, *127*, 11248–11249; d) E. R. King, E. T. Hennessy, T. A. Betley, *J. Am. Chem. Soc.* **2011**, *133*, 4917–4923; e) R. E. Cowley, N. A. Eckert, S. Vaddadi, T. M. Figg, T. R. Cundari, P. L. Holland, *J. Am. Chem. Soc.* **2011**, *133*, 9796–9811; f) E. R. King, G. T. Sazama, T. A. Betley, *J. Am. Chem. Soc.* **2012**, *134*, 17858–17861; g) L. Zhang, Y. Liu, L. Deng, *J. Am. Chem. Soc.* **2014**, *136*, 15525–15528; h) J. Du, L. Wang, M. Xie, L. Deng, *Angew. Chem. Int. Ed.* **2015**, *54*, 12640–12644; *Angew. Chem.* **2015**, *127*, 12831–12835.

[4] a) Y.-Y. Zhou, D. R. Hartline, T. J. Steiman, P. E. Fanwick, C. Uyeda, *Inorg. Chem.* **2014**, *53*, 11770–11777; b) T. J. Steiman, C. Uyeda, *J. Am. Chem. Soc.* **2015**, *137*, 6104–6110; c) S. Pal, C. Uyeda, *J. Am. Chem. Soc.* **2015**, *137*, 8042–8045.

[5] a) A. W. Pierpont, T. R. Cundari, *Inorg. Chem.* **2010**, *49*, 2038–2046; b) O. A. Olatunji-Ojo, T. R. Cundari, *Inorg. Chem.* **2013**, *52*, 8106–8113.

[6] A. C. Bowman, C. Milsmann, E. Bill, Z. R. Turner, E. Lobkovsky, S. DeBeer, K. Wieghardt, P. J. Chirik, *J. Am. Chem. Soc.* **2011**, *133*, 17353–17369.

[7] a) C. A. Laskowski, A. J. M. Miller, G. L. Hillhouse, T. R. Cundari, *J. Am. Chem. Soc.* **2011**, *133*, 771–773; b) D. E. Herbert, N. C. Lara, T. Agapie, *Chem. Eur. J.* **2013**, *19*, 16453–16460.

[8] C. A. Laskowski, G. L. Hillhouse, *Organometallics* **2009**, *28*, 6114–6120.

[9] S. Wiese, M. J. B. Aguila, E. Kogut, T. H. Warren, *Organometallics* **2013**, *32*, 2300–2308.

[10] a) B. J. Stokes, K. J. Richert, T. G. Driver, *J. Org. Chem.* **2009**, *74*, 6442–6451; b) W. G. Shou, J. Li, T. Guo, Z. Lin, G. Jia, *Organometallics* **2009**, *28*, 6847–6854; c) I. T. Alt, B. Plietker, *Angew. Chem. Int. Ed.* **2016**, *55*, 1519–1522; *Angew. Chem.* **2016**, *128*, 1542–1545.

[11] J. L. Bennett, P. T. Wolczanski, *J. Am. Chem. Soc.* **1997**, *119*, 10696–10719.

[12] a) P. J. Walsh, F. J. Hollander, R. G. Bergman, *J. Am. Chem. Soc.* **1988**, *110*, 8729–8731; b) C. C. Cummins, S. M. Baxter, P. T. Wolczanski, *J. Am. Chem. Soc.* **1988**, *110*, 8731–8733; c) C. P. Schaller, C. C. Cummins, P. T. Wolczanski, *J. Am. Chem. Soc.* **1996**, *118*, 591–611.

[13] For examples of catalytic carbazole syntheses by means of C–H amination, see: a) J. Jiao, K. Murakami, K. Itami, *ACS Catal.* **2016**, *6*, 610–633; b) W. C. P. Tsang, N. Zheng, S. L. Buchwald, *J. Am. Chem. Soc.* **2005**, *127*, 14560–14561; c) J. A. Jordan-Hore, C. C. C. Johansson, M. Gulias, E. M. Beck, M. J. Gaunt, *J. Am. Chem. Soc.* **2008**, *130*, 16184–16186; d) K. Takamatsu, K. Hirano, T. Satoh, M. Miura, *Org. Lett.* **2014**, *16*, 2892–2895.

[14] Reacting *m*-terphenylazide at 110 °C for 24 h in the presence of **1** (20 mol%) provides the carbazole product **8** in 49% yield. A k_H/k_D value of 4.5 was determined using *m*-[D_5]terphenylazide as a substrate.

Manuscript received: April 26, 2017

Accepted manuscript online: April 28, 2017

Version of record online: May 22, 2017